

Journal of  
**Photonics for Energy**

SPIEDigitalLibrary.org/jpe

**Toward bulk heterojunction polymer  
solar cells with thermally stable  
active layer morphology**

Ilaria Cardinaletti  
Jurgen Kesters  
Sabine Bertho  
Bert Conings  
Fortunato Piersimoni  
Jan D'Haen  
Laurence Lutsen  
Milos Nesladek  
Bruno Van Mele  
Guy Van Assche  
Koen Vandewal  
Alberto Salleo  
Dirk Vanderzande



**SPIE**

# Toward bulk heterojunction polymer solar cells with thermally stable active layer morphology

Ilaria Cardinaletti,<sup>a,\*</sup> Jurgen Kesters,<sup>a</sup> Sabine Bertho,<sup>a</sup> Bert Conings,<sup>a</sup> Fortunato Piersimoni,<sup>b</sup> Jan D'Haen,<sup>a</sup> Laurence Lutsen,<sup>c</sup> Milos Nesladek,<sup>a</sup> Bruno Van Mele,<sup>d</sup> Guy Van Assche,<sup>d</sup> Koen Vandewal,<sup>e</sup> Alberto Salleo,<sup>f</sup> Dirk Vanderzande,<sup>a,c</sup> Wouter Maes,<sup>a,c</sup> and Jean V. Manca<sup>a,c</sup>

<sup>a</sup>Hasselt University, Institute for Materials Research (IMO-IMOMEC),  
Wetenschapspark 1, Diepenbeek 3590, Belgium

<sup>b</sup>Universität Potsdam, Institut für Physik und Astronomie, Potsdam-Golm 14476, Germany

<sup>c</sup>IMEC vzw, Associated Lab IMOMEC, Diepenbeek 3590, Belgium

<sup>d</sup>Vrije Universiteit, Physical Chemistry and Polymer Science,  
Faculty of Engineering Sciences, Brussels 1050, Belgium

<sup>e</sup>Technische Universität, Institut für Angewandte Photophysik, Dresden 01069, Germany

<sup>f</sup>Stanford University, Department of Materials Science and Engineering,  
Stanford, California 94305

**Abstract.** When state-of-the-art bulk heterojunction organic solar cells with ideal morphology are exposed to prolonged storage or operation at elevated temperatures, a thermally induced disruption of the active layer blend can occur, in the form of a separation of donor and acceptor domains, leading to diminished photovoltaic performance. Toward the long-term use of organic solar cells in real-life conditions, an important challenge is, therefore, the development of devices with a thermally stable active layer morphology. Several routes are being explored, ranging from the use of high glass transition temperature, cross-linkable and/or side-chain functionalized donor and acceptor materials, to light-induced dimerization of the fullerene acceptor. A better fundamental understanding of the nature and underlying mechanisms of the phase separation and stabilization effects has been obtained through a variety of analytical, thermal analysis, and electro-optical techniques. Accelerated aging systems have been used to study the degradation kinetics of bulk heterojunction solar cells *in situ* at various temperatures to obtain aging models predicting solar cell lifetime. The following contribution gives an overview of the current insights regarding the intrinsic thermally induced aging effects and the proposed solutions, illustrated by examples of our own research groups. © The Authors. Published by SPIE under a Creative Commons Attribution 3.0 Unported License. Distribution or reproduction of this work in whole or in part requires full attribution of the original publication, including its DOI. [DOI: [10.1117/1.JPE.4.040997](https://doi.org/10.1117/1.JPE.4.040997)]

**Keywords:** organic photovoltaics; bulk heterojunction; thermal stability; phase separation; lifetime.

Paper 14009MV received Mar. 1, 2014; revised manuscript received Apr. 11, 2014; accepted for publication May 5, 2014; published online Jun. 10, 2014.

## 1 Introduction

In the last decades, organic bulk heterojunction (BHJ) solar cells have gradually evolved from a purely academic research topic to a promising emerging technology with world-wide R&D activities. With the first commercial applications on the market (e.g., the solar bags of Neuber<sup>1</sup>) and efficiencies reaching >10%,<sup>2</sup> the lifetime of the devices (predicted to be several years<sup>3</sup>) becomes important. In order to test the durability of solar cells during operation, a variety of stress factors must be considered, such as humidity and oxidizing agents in ambient atmosphere, incident ultraviolet (UV), and visible radiation, and the high temperatures reached after prolonged exposure to sunlight. Since gathering fundamental knowledge on these degradation

\*Address all correspondence to: Ilaria Cardinaletti, E-mail: [ilaria.cardinaletti@uhasselt.be](mailto:ilaria.cardinaletti@uhasselt.be)

processes represents an important step toward the realization of more durable devices, various laboratories are investigating them and have agreed on testing protocols that allow for an easier comparison of results among different groups.<sup>4</sup> Regarding the failure mechanisms in BHJ organic photovoltaics, several review papers can be found.<sup>5–7</sup> Herein, we restrict ourselves to a brief overview of some of the most reported causes of losses in power conversion efficiencies (Table 1).

Reversible degradation can occur due to oxygen doping of some metal oxides, widely employed as interfacial layers between the BHJ and the cathode.<sup>7</sup> On the other hand, exposure to light accelerates the reversible p-doping of the polymer as it absorbs oxygen from the atmosphere, with a resulting decrease in short-circuit current density ( $J_{sc}$ ).<sup>6,10</sup> Alongside these effects, other mechanisms lead to irreversible degradation and fatal device failure. The ingress of water into the device can cause fast oxidation of the low-work function metal cathode (Yb, Ca, Al).<sup>8</sup> Moreover, oxygen was found to promote the rupture of the  $\pi$ -conjugated backbone in the electron donor polymer within the active blend under UV illumination, with a subsequent drop in absorbance. This phenomenon is less effective in the presence of a fullerene derivative,<sup>6</sup> such as the most widely used acceptor material, [6,6]-phenyl-C<sub>61</sub>-butyric acid methyl ester (PCBM).

Some of these issues can be prevented by appropriate encapsulation<sup>14</sup> and can, thus, be considered as extrinsic degradation mechanisms.<sup>15,16</sup> Next to extrinsic failures, a variety of intrinsic failure mechanisms, linked directly to the properties of the materials used (as further defined in Ref. 16), may also occur. Table 1 provides a selection of the important extrinsic and intrinsic degradation phenomena observed in organic solar cells.

In this contribution, we focus on one particular intrinsic failure mechanism: the thermally induced disruption of the active layer blend (nano) morphology of polymer:fullerene BHJ organic solar cells (Fig. 1). During thermal annealing, the BHJ system gains energy, which allows it to order itself in a more thermodynamically stable way. This leads to a thermally induced separation of the polymer and fullerene phases. As a result, small PCBM crystals tend to group into larger crystalline domains, a phenomenon called Ostwald ripening.<sup>14,17</sup> The formation of these PCBM-rich features leads to a decrease of the interfacial area between donor and acceptor and, thus, to a diminution of exciton dissociation and of the number of percolation paths to the electrodes.<sup>6</sup> In this phase separation phenomenon, the glass transition temperature ( $T_g$ ) of the blend plays an important role.<sup>18</sup> Above  $T_g$ , the blend component molecules become mobile, which allows diffusion and clustering of the fullerene derivatives.

Better insights regarding the nature of the phase separation process have been obtained through a variety of characterization methods. In the next paragraph, we provide a short overview of the analytical, thermal analysis and electro-optical techniques used to investigate the morphology of BHJ active layers at their initial stage as well as during and after thermal stress. Subsequently, the effects of thermally induced morphological changes on the photovoltaic properties are described. Models to predict the impact of structural degradation are introduced, together with analyses of its impact on the durability of the devices. Finally, we introduce various routes proposed to improve the thermal stability of the active layer blend morphology, such as the use of high- $T_g$  polymers, the addition of

**Table 1** Extrinsic and intrinsic degradation mechanisms in organic solar cells.

Extrinsic degradation	Intrinsic degradation
• Electrode oxidation <sup>8</sup>	• Phase separation of the polymer:fullerene blend <sup>9</sup>
• Photo-oxidation of the conjugated polymer/ small molecule <sup>10</sup>	• Material diffusion from the electrodes into the active layer <sup>11</sup>
• Reversible oxygen-doping of interfacial metal oxides <sup>12</sup>	• Reversible charge accumulation at the interfaces with the electrodes after light exposure <sup>13</sup>
• Reversible p-doping of the photoactive layer due to oxygen <sup>10</sup>	

functionalized/thermo-cleavable side-chains, cross-linking, or the photo-induced dimerization of the fullerene component.

## 2 Characterization of the BHJ Blend Stabil

### 2.1 Investigation of the Active Layer Morphology

The stability of the active layer blend morphology is crucial for the long-term operation of the solar cells. Optimal intermixing requires that the distance between the domain interfaces of the polymer and fullerene materials does not exceed the exciton diffusion length, typically in the order of 10 nm.<sup>15</sup> A variety of techniques have been employed to determine on which length scale the intermixing occurs. Optical microscopy can be used to study the presence of large structures in the active layer film. Information on their height is obtained via stylus profilometry or atomic force microscopy (AFM) for micro- and nanoscale features, respectively.<sup>19,20</sup> AFM represents a valuable tool to analyze the film topography,<sup>21</sup> and it also enables one to distinguish structures from the different components in the blend through peak force tapping<sup>22</sup> and conductive-AFM.<sup>22,23</sup> Scanning electron microscopy (SEM)<sup>24</sup> and transmission electron microscopy (TEM)<sup>20</sup> techniques are used to image thin layers of organic semiconductors as well. Electron tomography reconstructions of three-dimensional volumes,<sup>25</sup> together with cross-sectional SEM and TEM,<sup>6</sup> allow the investigation of the vertical disposition of donor-acceptor domains throughout a layer<sup>2,25</sup> or throughout a cross-section of a device.<sup>21</sup> Figure 2 (top row) shows an example of the evolution of the morphology of a poly[2-methoxy-5-(3',7'-dimethyloctyloxy)-1,4-phenylene vinylene] (MDMO-PPV): PCBM (1:4 wt%) blend after various durations of thermal annealing at 110°C (above the  $T_g$  of the blend), as visualized by TEM. It is clearly observed that the initially finely dispersed phases rapidly evolve toward the formation of aggregated structures, identified as PCBM domains. Due to the thermal treatment, the PCBM molecules diffuse out of the originally intermixed photoactive layer and aggregate into large domains. This Ostwald ripening (Fig. 1) is observed for numerous polymer:fullerene blends.<sup>20,21,24</sup>

Diffraction studies can also provide information on ordered structures in BHJ films. Selected-area electron diffraction (SAED) allows attributing the observed structures to specific blend components.<sup>20,27</sup> X-ray diffraction measurements enable determination of the nature of the crystalline structures.<sup>23</sup> In grazing-incidence geometry, information is obtained on the ordering and orientation of crystallites and crystalline planes in a thin film<sup>2,27</sup> or on the stacking of the  $\pi$ -chains in largely amorphous materials.<sup>28</sup> As an illustration of the use of diffraction techniques in the study of thermally induced Ostwald ripening in BHJ organic solar cells, the insets of Fig. 2 (top row) show the crystalline nature of the PCBM aggregates formed during thermal annealing, as identified via SAED.

Together with UV-visible absorption<sup>29,30</sup> and Raman spectroscopy,<sup>29</sup> these microscopy and diffraction techniques can be used to determine the initial morphology of BHJ active layers<sup>21</sup> as well as the changes in the blend structures due to annealing treatments<sup>23,27</sup> or aging of the film.<sup>6,14</sup>

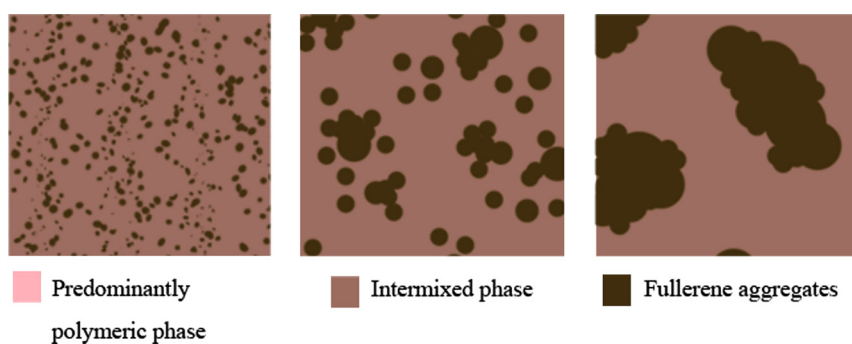


**Fig. 1** Schematics of the evolution of fullerene aggregation in thermally annealed bulk heterojunction organic solar cells.

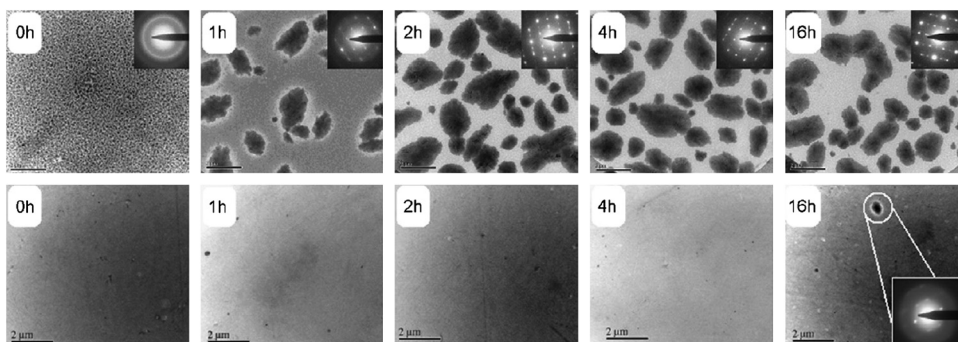


**Fig. 2** Transmission electron microscopy (TEM) images of poly[2-methoxy-5-(3',7'-dimethyloctyloxy)-1,4-phenylene vinylene] (MDMO-PPV): [6,6]-phenyl-C<sub>61</sub>-butyric acid methyl ester (PCBM) (1:4) (top) and high-T<sub>g</sub> PPV: PCBM (bottom) blend films after various annealing times at 110°C. The selected-area electron diffraction (SAED) insets show the crystalline nature of the aggregates. Reprinted from Ref. 26, with permission from Elsevier.

## 2.2 Thermal Analysis

It is nowadays recognized that a physicochemical approach based on dedicated thermal analysis protocols can strongly contribute to an increased understanding of (nano) morphology development and stabilization in BHJ organic solar cell blends. Calorimetric techniques, such as differential scanning calorimetry (DSC),<sup>31–35</sup> modulated DSC (Ref. 32), and especially rapid heat-cool calorimetry,<sup>18</sup> allow characterization of both ordered and disordered material phases and determination of phase/state diagrams. The state diagram for the donor-acceptor system is of primordial importance for a systematic understanding of the phase-separation behavior and for designing appropriate thermal annealing and accelerated aging procedures (see also Sec. 3.1). In this respect, the crystallization kinetics of the crystallizable component(s) as a function of temperature in the temperature window of interest is indispensable.<sup>18</sup> In the state diagram of poly(3-hexylthiophene) (P3HT):PCBM, for example, the glass transition of PCBM (ca. 140°C) and the role of mobility restrictions by (partial) vitrification was demonstrated.<sup>32</sup> The results reported are in line with actual statements regarding the importance of disorder and the amorphous phase in the active layer.<sup>36</sup> In addition, the state diagram also permits the detection of the presumed eutectic phase behavior, with a finely intermixed morphology of donor and acceptor constituents, which might lead to an efficient thermal procedure to predict/propose mixing conditions of new blends for optimum solar cell performance.<sup>31,33–35</sup>

## 3 Effect of Active Layer Morphology Degradation on Photovoltaic Properties

As illustrated above, annealing at high temperatures promotes morphological rearrangement in BHJ blends because of the available thermal energy. The new phase distribution can have specific effects on the final photovoltaic performance of the devices, depending on the nature of the components. When a partially crystalline polymer (such as P3HT) is mixed with PCBM, an increase in hole mobility is reached by thermal annealing, as the latter promotes a strengthening of the crystalline character of the polymer.<sup>23</sup> Concurrently, high temperatures induce PCBM aggregation. As a consequence, systems of this sort show an optimal annealing approach, which allows for high mobility in the crystalline polymer, but beyond which the formation of large PCBM domains causes a decrease in performance.<sup>23</sup> On the other hand, when there is no ideal crystalline structure to be reached, as in the case of largely amorphous polymers, thermal annealing above the T<sub>g</sub> of the blend leads to the formation of fullerene clusters only.<sup>17,37</sup> In the following section, it will be shown that these thermally induced morphological changes influence the short-circuit current density, the fill factor (FF), and the open-circuit voltage (V<sub>oc</sub>), thus altering the final photovoltaic energy conversion efficiency.

### 3.1 Effect of Morphology Degradation on $J_{sc}$

The formation of aggregates of fullerene derivatives in BHJ films leads to a deterioration of the  $J_{sc}$  of the devices, partially due to a reduction of the interfacial area between the donor and acceptor domains, and partially due to the diminution of the photoactive area.<sup>38</sup> For organic BHJ solar cells, it has been reported by several authors that the short-circuit current density ( $J_{sc}$ ) decreases upon prolonged annealing and that the degradation occurs at a faster rate when higher annealing temperatures are applied.<sup>9,26</sup> In blends of MDMO-PPV with PCBM, the degradation curves for  $J_{sc}$  have been fitted with Eq. (1) to reflect the Ostwald ripening occurring in the active layer during annealing<sup>17</sup>

$$J_{sc}(t) = J_{sc}(\infty) + J_{sc}(0) \exp(-k_{deg}\sqrt{t}). \quad (1)$$

In Eq. (1),  $t$  represents the annealing time and  $k_{deg} = A \exp(-E_a/k_B T)$  is a rate constant that characterizes how fast the degradation evolves, with  $E_a$  the activation energy in eV,  $k_B$  the Boltzmann constant ( $8.62 * 10^{-5}$  eV K<sup>-1</sup>), and  $A$ , a constant that depends on the degradation mechanisms and the experimental conditions. Figure 3 shows the fitted curves (solid lines) and the measured decay in short circuit current at different annealing temperatures.

A similar approach was proposed to predict the lifetime of devices using the Lipshitz-Slyozov theory for spinodal decomposition, which predicts domain-size ( $R$ ) evolution following  $R \sim t^n$ , with  $n$  a material-dependent exponent,<sup>39</sup> stressing the strong relationship between the employed polymer:fullerene system and its inherent rate of morphological degradation.

The link between the rearrangement of the active blend's structure on the nanoscale and the drop in  $J_{sc}$  has also been investigated by Schaffer et al.<sup>38</sup> through the acquisition of  $I$ - $V$  characteristics and *in situ* micro-focused grazing incidence small-angle x-ray scattering ( $\mu$ GISAXS) patterns of P3HT:PCBM devices during operation. They documented the change in P3HT domain size and density within the active layer blend matrix and introduced a model to quantitatively determine the  $J_{sc}$  of a device from the recorded morphology data by correlating the active interfacial area between the two species in the blend with the dimension of the structures, as measured with  $\mu$ GISAXS.

### 3.2 Effect of Morphological Degradation on Other Photovoltaic Parameters

Thermal annealing not only has an effect on  $J_{sc}$ , but it also influences the open-circuit voltage and FF. It was reported that the nanomorphology of the active layer plays a significant role in the determination of  $V_{oc}$ <sup>40,41</sup> due to the correlation between the latter and the energy ( $E_{CT}$ ) of the interfacial donor-acceptor charge transfer complex (CTC).<sup>42,43</sup>  $E_{CT}$  can be determined through modeling the sub-bandgap photocurrent spectra,<sup>44</sup> as measured by Fourier-transform photocurrent spectroscopy, an ultrasensitive technique that allows one to measure the external quantum efficiency over nine orders of magnitude.<sup>45</sup> Given the reported linear relation between  $E_{CT}$  and  $V_{oc}$ , the variation of  $E_{CT}$  during the aging process was studied to understand the origin of

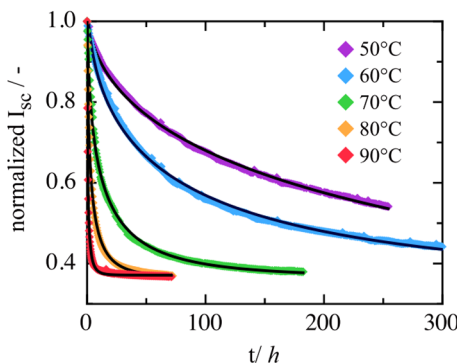


**Fig. 3** Simulated curves matching well with the drop in short-circuit current ( $I_{sc}$ ) of MDMO-PPV:PCBM solar cells upon thermal annealing. Reproduced with permission from Ref. 17.

the drop in  $V_{oc}$  upon morphological reorganization.<sup>41,43,46,47</sup> Thermally annealed MDMO-PPV:PCBM devices showed a reduction of  $V_{oc}$  and  $E_{CT}$ , with the PCBM photocurrent peak at 1.74 eV becoming more prominent due to the formation of PCBM aggregates and the amount of interfacial CTCs decreasing. This indicates less interaction between the donor and acceptor and, thus, a more phase-separated BHJ blend morphology.<sup>35</sup> A more detailed discussion on the effect of structural factors on  $V_{oc}$ ,  $E_{CT}$ , and photovoltaic performance in organic solar cells is given in a recent paper by Vandewal et al.<sup>48</sup>

FF is also observed to change in relation to reorganizations of the materials at the nanoscale.<sup>23</sup> The optimal morphology of the BHJ photoactive layer blends ensures good percolation paths from the exciton dissociation site to the collecting electrodes.<sup>49</sup> When the mixing of donor and acceptor domains is not optimal any more, as in the case of thermally degraded devices, the number of percolation paths is reduced and the series resistance of the devices increases, which leads to a decrease of FF.<sup>49</sup>

#### 4 Methods to Stabilize the BHJ Active Layer Morphology

Thermally induced structural changes in BHJ active layers at operating temperatures represent an intrinsic limit to the employability of certain material systems in outdoor conditions,<sup>15</sup> in which temperatures  $>100^{\circ}\text{C}$  can be reached (temperatures up to  $175^{\circ}\text{C}$  were measured for silicon modules in Arizona<sup>50</sup>). For this reason, we dedicate this section to some of the methods that have been proposed to improve the morphological stability of photoactive material blends.<sup>6</sup>

A careful choice of the donor-acceptor ratio<sup>51</sup> and the casting solvent can result in not only more efficient,<sup>52</sup> but also more durable organic solar cells.<sup>30</sup> Depositing photoactive layers via different solvents was demonstrated to dictate the  $T_g$  and the ordering of the  $\pi\text{-}\pi$  stacking in amorphous poly[*N*-9''-heptadecanyl-2,7-carbazole-*alt*-5,5-(4',7'-di-2-thienyl-2',1',3'-benzo-thiadiazole)] (PCDTBT):[6,6]-phenyl-C<sub>71</sub>-butyric acid methyl ester (PC<sub>70</sub>BM) blends.<sup>37,53</sup> This system, stable at outdoor solar cell operating temperatures, thanks to its high  $T_g$  ( $\sim 130^{\circ}\text{C}$ ),<sup>37</sup> needs to be optimized through processing conditions<sup>52</sup> or solvent annealing<sup>54</sup> and has been determined to reach an extrapolated lifetime of seven years.<sup>3</sup> Removing residual solvents by treating the layers with methanol also proved to reduce thermally induced fullerene aggregation.<sup>55</sup> Additionally, a lower regioregularity and higher purity of the donor polymers, as well as the addition of block copolymer compatibilizers, has also been demonstrated to result in more stable films.<sup>5,56-58</sup>

It was shown that employing polymers with a  $T_g$  higher than the temperature agreed on for standard testing [ $85^{\circ}\text{C}$  (Ref. 4)] helps to slow down PCBM clustering over the lifetime of the solar cells, due to the high rigidity of the polymer chains in said conditions.<sup>6,26,59</sup> An example is shown in Fig. 2 (bottom row), where TEM analysis indicates that the employment of a high- $T_g$  PPV polymer results in a more thermally stable blend as compared to standard MDMO-PPV. A similar comparison was reported by Vandenbergh et al. (poly[2-methoxy-5-(2'-phenylethoxy)-1,4-phenylene vinylene] versus MDMO-PPV).<sup>60</sup> A high  $T_g$  also ensures stability of the electronic properties of (semicrystalline) polymers.<sup>53</sup>

A number of research groups have investigated the effect of polymer side-chain substitution on the blend stability.<sup>61-65</sup> Kesters et al.<sup>66</sup> showed that the introduction of a small amount (5 to 15%) of functionalized side-chains in poly(3-alkylthiophene) (P3AT) copolymers results in a considerably increased blend stability upon prolonged thermal stress. Devices employing functionalized P3AT copolymers in blends with PCBM showed initial efficiencies comparable to regular P3HT:PCBM solar cells and drastically reduced fullerene aggregation at the ISOS-3 standard testing temperature of  $85^{\circ}\text{C}$  for a timescale of 700 h.<sup>4</sup> Figure 4 illustrates TEM images of functionalized P3AT copolymer:PCBM blends after different thermal annealing times (in comparison with standard P3HT:PCBM). SAED allowed identifying the formed clusters as PCBM crystals.

The use of block copolymers containing both donor and acceptor domains has also been proposed as a strategy to improve photoactive layer stability,<sup>67</sup> although their synthesis remains challenging.<sup>7</sup> In these compounds, the donor and acceptor phases are covalently linked, allowing the material to be employed in single-component organic solar cells with stable morphology.

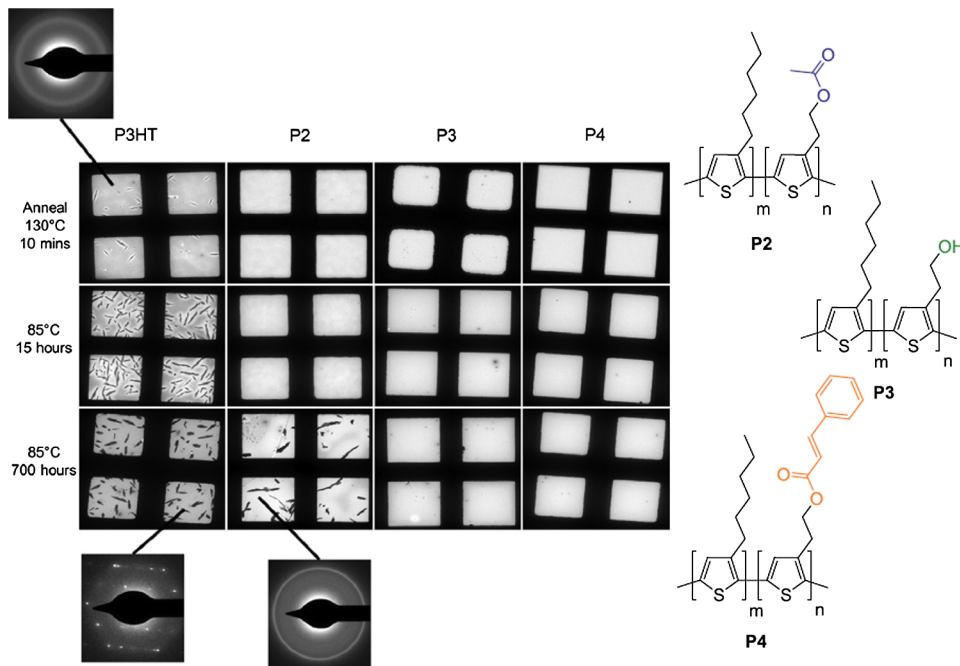


**Fig. 4** TEM images and SAED patterns of polymer (P2 to P4): PCBM (1:1) blends degraded at high temperature. Reprinted with permission from Ref. 66.

Furthermore, rigid polymers can also be obtained by thermal cleaving of the side-chains, introduced to ensure good solubility but, in principle, not needed for optoelectronic functionality. This strategy has also been proven to lead to morphologically stable BHJ films.<sup>59</sup>

Another popular strategy uses cross-linking of the active materials, either via polymer or fullerene component, to freeze in the optimal morphology. This can, for instance, be achieved by adding cross-linkable groups to the polymer side-chains<sup>68</sup> and curing the film with UV light. The employment of a cross-linked fullerene derivative, aligned in vertical nanorods, achieving a (quasi)ordered organic/organic nanostructure, allowed for an improved thermal stability, as well.<sup>69</sup>

Modifying the nature or the number of side-chains on the fullerene results in more amorphous compounds,<sup>55,70</sup> which can also lead to an improved morphological stability. Liao et al. were able to exploit supramolecular interactions to impose a given order to the BHJ film and ensure structural firmness.<sup>71</sup> They introduced a fullerene derivative, [6,6]-phenyl-C<sub>61</sub>-butyric acid pentafluorophenyl ester (PCBP<sup>F</sup>), in which the methyl group of PCBM is substituted by a pentafluorophenyl ring, and then exploited the known interaction between C<sub>60</sub> and the pentafluorophenyl moiety to produce solar cells with enhanced high-temperature stability.

Piersimoni et al.<sup>20</sup> and Li et al.<sup>72</sup> demonstrated the stabilizing effect of fullerene photodimerization on the active layer blend morphology. Light soaking of polymer:PCBM films before or during annealing above the T<sub>g</sub> of the blend resulted in reduced fullerene aggregation, although the effect becomes less appreciable with increasing temperatures<sup>20</sup> due to thermally induced dissociation of the dimers. These experiments were conducted using either PCBM or PC<sub>70</sub>BM, in combination with MDMO-PPV, P3HT, and PCDTBT as donor polymers (annealing the latter at higher temperature because of the elevated T<sub>g</sub> of the polymer). Optical microscopy images, shown in Fig. 5, confirmed that thermal aging in the dark promotes the formation of clusters, attributed to the PCBM, while the same treatment under illumination does not significantly affect the morphology of the BHJ layers. While these images prove the stabilizing effect of this photoreaction on the blends' morphology, its impact on the performance of devices resulted strongly system-dependent. Indeed, it can contribute to raising the J<sub>sc</sub> in PCDTBT-based solar cells,<sup>72</sup> but it was also reported by other authors to be responsible for performance degradation when combined with a bithiophene-co-thiazolothiazole push-pull copolymer.<sup>73</sup>

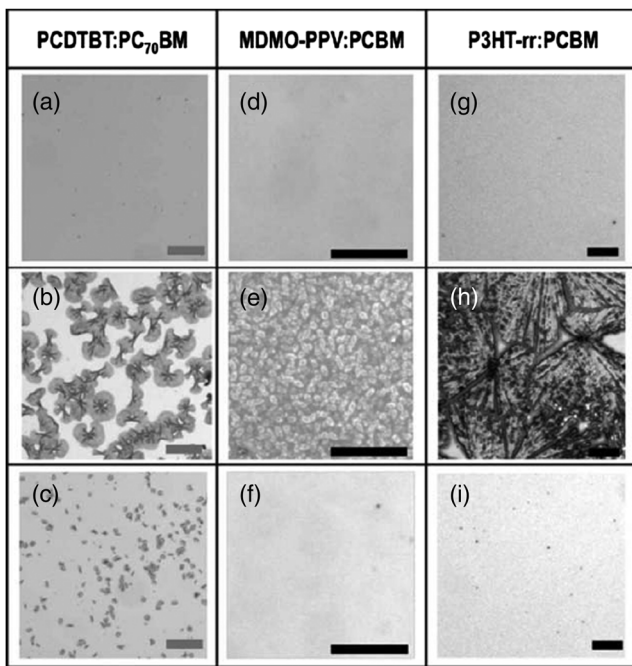


**Fig. 5** Comparison between optical reflection microscopy images of as-cast films (top row), films annealed at 180°C (b), and 110°C [(e) and (h)] in the dark, and films annealed at the same temperatures under solar illumination. Reproduced with permission from Ref. 20.

## 5 Conclusions and Outlook

Prolonged storage or operation of polymer:fullerene BHJ organic solar cells can result in athermally induced disruption of the optimal photoactive layer morphology via phase separation and Ostwald ripening of the fullerene domains, leading to a significant reduction of the photovoltaic performance. Improving the morphological stability of the photoactive blends upon thermal stress is, therefore, an important challenge for future commercialization of these devices. We briefly reviewed the degradation mechanisms resulting in performance failure, as well as the main techniques employed to characterize the thermally induced changes in the active layer (nano)morphology. The most obvious indication for BHJ structural damage is the formation of large crystalline domains of the fullerene derivative, with a consequent reduction of the interfacial area between the donor and acceptor domains, and a consequent negative effect on the photovoltaic parameters. Insights on the underlying mechanisms provide the foundation to model the effect of this structural reorganization on the photovoltaic parameters, allowing the prediction of device lifetimes and degradation rates.

Toward more intrinsically stable BHJ organic solar cells, several roads have been proposed and are still under investigation, regarding the choice of materials, the exploitation of observed phenomena, and the modification of compounds. The reviewed solutions will undoubtedly continue to find their way toward the development of stable organic photovoltaic devices. On the other hand, dedicated thermal analysis of the blends, as well as accurate investigation of the morphological changes in degraded photoactive layers, can be regarded as valuable tools in the direction of intrinsically stable organic solar cells.

## Acknowledgments

The authors would like to acknowledge the Interreg-project ORGANEXT and the Fund for Scientific Research, Flanders (Belgium) (FWO) for the financial support.

## References

1. “Neuber products,” <http://www.energy-sunbags.de> (28 February 2014).

2. L. Dou et al., “25th anniversary article: a decade of organic/polymeric photovoltaic research,” *Adv. Mater.* **25**(46), 6642–6671 (2013), <http://dx.doi.org/10.1002/adma.v25.46>.
3. C. H. Peters et al., “High efficiency polymer solar cells with long operating lifetimes,” *Adv. Energy Mater.* **1**(4), 491–494 (2011), <http://dx.doi.org/10.1002/aenm.201100138>.
4. M. O. Reese et al., “Consensus stability testing protocols for organic photovoltaic materials and devices,” *Sol. Energy Mater. Sol. Cells* **95**(5), 1253–1267 (2011), <http://dx.doi.org/10.1016/j.solmat.2011.01.036>.
5. J. U. Lee et al., “Degradation and stability of polymer-based solar cells,” *J. Mater. Chem.* **22**(46), 24265–24283 (2012), <http://dx.doi.org/10.1039/c2jm33645f>.
6. N. Grossiord et al., “Degradation mechanisms in organic photovoltaic devices,” *Org. Electron.* **13**(3), 432–456 (2012), <http://dx.doi.org/10.1016/j.orgel.2011.11.027>.
7. M. Jørgensen et al., “Stability of polymer solar cells,” *Adv. Mater.* **24**(5), 580–612 (2012), <http://dx.doi.org/10.1002/adma.201104187>.
8. E. Voroshazi et al., “Influence of cathode oxidation via the hole extraction layer in polymer: fullerene solar cells,” *Org. Electron.* **12**(5), 736–744 (2011), <http://dx.doi.org/10.1016/j.orgel.2011.01.025>.
9. S. Bertho et al., “Influence of thermal ageing on the stability of polymer bulk heterojunction solar cells,” *Sol. Energy Mater. Sol. Cells* **91**(5), 385–389 (2007), <http://dx.doi.org/10.1016/j.solmat.2006.10.008>.
10. A. Seemann et al., “Reversible and irreversible degradation of organic solar cell performance by oxygen,” *Sol. Energy* **85**(6), 1238–1249 (2011), <http://dx.doi.org/10.1016/j.solener.2010.09.007>.
11. R. Steim, F. R. Kogler, and C. J. Brabec, “Interface materials for organic solar cells,” *J. Mater. Chem.* **20**(13), 2499–2512 (2010), <http://dx.doi.org/10.1039/b921624c>.
12. E. Voroshazi et al., “Role of electron and hole collecting buffer layers on the stability of inverted polymer: fullerene photovoltaic devices,” *J. Photovoltaics* **4**(1), 265–270 (2014), <http://dx.doi.org/10.1109/JPHOTOV.2013.2287913>.
13. K. Kawano and C. Adachi, “Evaluating carrier accumulation in degraded bulk heterojunction organic solar cells by a thermally stimulated current technique,” *Adv. Funct. Mater.* **19**(24), 3934–3940 (2009), [http://dx.doi.org/10.1002/\(ISSN\)1616-3028](http://dx.doi.org/10.1002/(ISSN)1616-3028).
14. P. Kumar and S. Chand, “Recent progress and future aspects of organic solar cells,” *Prog. Photovolt: Res. Appl.* **20**(4), 377–415 (2012), <http://dx.doi.org/10.1002/pip.v20.4>.
15. C. J. Brabec et al., “Polymer-fullerene bulk-heterojunction solar cells,” *Adv. Mater.* **22**(34), 3839–3856 (2010), <http://dx.doi.org/10.1002/adma.200903697>.
16. F. C. Krebs, *Stability and Degradation of Organic and Polymer Solar Cells*, Chapter 1, John Wiley & Sons, Chichester, West Sussex, United Kingdom (2012).
17. B. Conings et al., “Modeling the temperature induced degradation kinetics of the short circuit current in organic bulk heterojunction solar cells,” *Appl. Phys. Lett.* **96**(16), 163301 (2010), <http://dx.doi.org/10.1063/1.3391669>.
18. F. Demir et al., “Isothermal crystallization of P3HT: PCBM blends studied by RHC,” *J. Therm. Anal. Calorim.* **105**(3), 845–849 (2011), <http://dx.doi.org/10.1007/s10973-011-1701-8>.
19. O. Oklobia and T. S. Shafai, “A quantitative study of the formation of PCBM clusters upon thermal annealing of P3HT/PCBM bulk heterojunction solar cell,” *Sol. Energy Mater. Sol. Cells* **117**, 1–8 (2013), <http://dx.doi.org/10.1016/j.solmat.2013.05.011>.
20. F. Piersimoni et al., “Influence of fullerene photodimerization on the PCBM crystallization in polymer: fullerene bulk heterojunctions under thermal stress,” *J. Polym. Sci. B Polym. Phys.* **51**(16), 1209–1214 (2013), <http://dx.doi.org/10.1002/polb.v51.16>.
21. S. Kouijzer et al., “Predicting morphologies of solution processed polymer: fullerene blends,” *J. Am. Chem. Soc.* **135**(32), 12057–12067 (2013), <http://dx.doi.org/10.1021/ja405493j>.
22. S. Desbief et al., “Nanoscale investigation of the electrical properties in semiconductor polymer–carbon nanotube hybrid materials,” *Nanoscale* **4**(8), 2705–2712 (2012), <http://dx.doi.org/10.1039/c2nr11888b>.
23. X. Yan and A. Uddin, “Effect of thermal annealing on P3HT: PCBM bulk-heterojunction organic solar cells: a critical review,” *Renewable Sustainable Energy Rev.* **30**, 324–336 (2014), <http://dx.doi.org/10.1016/j.rser.2013.10.025>.

24. J. A. Moore, S. Ali, and B. C. Berry, "Stabilization of PCBM domains in bulk heterojunctions using polystyrene-tethered fullerene," *Sol. Energy Mater. Sol. Cells* **118**, 96–101 (2013), <http://dx.doi.org/10.1016/j.solmat.2013.07.044>.
25. B. V. Andersson et al., "Imaging of the 3D nanostructure of a polymer solar cell by electron tomography," *Nano Lett.* **9**(2), 853–855 (2009), <http://dx.doi.org/10.1021/nl803676e>.
26. S. Bertho et al., "Effect of temperature on the morphological and photovoltaic stability of bulk heterojunction polymer: fullerene solar cells," *Sol. Energy Mater. Sol. Cells* **92**(7), 753–760 (2008), <http://dx.doi.org/10.1016/j.solmat.2008.01.006>.
27. F. Liu et al., "Characterization of the morphology of solution-processed bulk heterojunction organic photovoltaics," *Prog. Polym. Sci.* **38**(12), 1990–2052 (2013), <http://dx.doi.org/10.1016/j.progpolymsci.2013.07.010>.
28. P. A. Staniec et al., "The nanoscale morphology of a PCDTBT: PCBM photovoltaic blend," *Adv. Energy Mater.* **1**(4), 499–504 (2011), <http://dx.doi.org/10.1002/aenm.201100144>.
29. P. Veerender et al., "Probing the annealing induced molecular ordering in bulk heterojunction polymer solar cells using in-situ Raman spectroscopy," *Sol. Energy Mater. Sol. Cells* **120**, 526–535 (2014), <http://dx.doi.org/10.1016/j.solmat.2013.09.034>.
30. L. Chang et al., "Correlating dilute solvent interactions to morphology and OPV device performance," *Org. Electron.* **14**(10), 2431–2443 (2013), <http://dx.doi.org/10.1016/j.orgel.2013.06.016>.
31. C. Müller et al., "Binary organic photovoltaic blends: a simple rationale for optimum compositions," *Adv. Mater.* **20**(18), 3510–3515 (2008), <http://dx.doi.org/10.1002/adma.200800963>.
32. J. Zhao et al., "Phase diagram of P3HT / PCBM blends and its implication for the stability of morphology," *J. Phys. Chem. B* **113**(6), 1587–1591 (2009), <http://dx.doi.org/10.1021/jp804151a>.
33. C. Nicolet et al., "Optimization of the bulk heterojunction composition for enhanced photovoltaic properties: correlation between the molecular weight of the semiconducting polymer and device performance," *J. Phys. Chem. B* **115**(44), 12717–12727 (2011), <http://dx.doi.org/10.1021/jp207669j>.
34. N. Li et al., "Determination of phase diagrams of binary and ternary organic semiconductor blends for organic photovoltaic devices," *Sol. Energy Mater. Sol. Cells* **95**(12), 3465–3471 (2011), <http://dx.doi.org/10.1016/j.solmat.2011.08.005>.
35. A. A. Y. Guilbert et al., "Effect of multiple adduct fullerenes on microstructure and phase behavior of P3HT: fullerene blend films for organic solar cells," *ACS Nano* **6**(5), 3868–3875 (2012), <http://dx.doi.org/10.1021/nn204996w>.
36. R. Noriega et al., "A general relationship between disorder, aggregation and charge transport in conjugated polymers," *Nat. Mater.* **12**(11), 1037–1043 (2013), <http://dx.doi.org/10.1038/nmat3722>.
37. T. Wang et al., "Correlating structure with function in thermally annealed PCDTBT: PC 70 BM photovoltaic blends," *Adv. Funct. Mater.* **22**(7), 1399–1408 (2012), <http://dx.doi.org/10.1002/adfm.v22.7>.
38. C. J. Schaffer et al., "A direct evidence of morphological degradation on a nanometer scale in polymer solar cells," *Adv. Mater.* **25**(46), 6760–6764 (2013), <http://dx.doi.org/10.1002/adma.v25.46>.
39. B. Ray and M. A. Alam, "A compact physical model for morphology induced intrinsic degradation of organic bulk heterojunction solar cell," *Appl. Phys. Lett.* **99**(3), 033303 (2011), <http://dx.doi.org/10.1063/1.3610460>.
40. F. Piersimoni et al., "Influence of fullerene ordering on the energy of the charge-transfer state and open-circuit voltage in polymer: fullerene solar cells," *J. Phys. Chem. C* **115**(21), 10873–10880 (2011), <http://dx.doi.org/10.1021/jp110982m>.
41. K. Vandewal et al., "The relation between open-circuit voltage and the onset of photocurrent generation by charge-transfer absorption in polymer: fullerene bulk heterojunction solar cells," *Adv. Funct. Mater.* **18**(14), 2064–2070 (2008), <http://dx.doi.org/10.1002/adfm.v18.14>.
42. K. Tvingstedt et al., "Electroluminescence from charge transfer states in polymer solar cells," *J. Am. Chem. Soc.* **131**(33), 11819–11824 (2009), <http://dx.doi.org/10.1021/ja903100p>.

43. M. Hallermann, S. Haneder, and E. Da Como, "Charge-transfer states in conjugated polymer/fullerene blends: below-gap weakly bound excitons for polymer photovoltaics," *Appl. Phys. Lett.* **93**(5), 053307 (2008), <http://dx.doi.org/10.1063/1.2969295>.
44. K. Vandewal et al., "Relating the open-circuit voltage to interface molecular properties of donor: acceptor bulk heterojunction solar cells," *Phys. Rev. B* **81**(12), 12520 (2010), <http://dx.doi.org/10.1103/PhysRevB.81.125204>.
45. K. Vandewal et al., "Fourier-transform photocurrent spectroscopy for a fast and highly sensitive spectral characterization of organic and hybrid solar cells," *Thin Solid Films* **516**(20), 7135–7138 (2008), <http://dx.doi.org/10.1016/j.tsf.2007.12.056>.
46. L. Goris et al., "Observation of the subgap optical absorption in polymer-fullerene blend solar cells," *Appl. Phys. Lett.* **88**(5), 052113 (2006), <http://dx.doi.org/10.1063/1.2171492>.
47. B. P. Rand, D. P. Burk, and S. R. Forrest, "Offset energies at organic semiconductor heterojunctions and their influence on the open-circuit voltage of thin-film solar cells," *Phys. Rev. B* **75**(11), 115327 (2007), <http://dx.doi.org/10.1103/PhysRevB.75.115327>.
48. K. Vandewal, S. Himmelberger, and A. Salleo, "Structural factors that affect the performance of organic bulk heterojunction solar cells," *Macromolecules* **46**(16), 6379–6387 (2013), <http://dx.doi.org/10.1021/ma400924b>.
49. B. Ray and M. A. Alam, "Random vs regularized OPV: limits of performance gain of organic bulk heterojunction solar cells by morphology engineering," *Sol. Energy Mater. Sol. Cells* **99**, 204–212 (2012), <http://dx.doi.org/10.1016/j.solmat.2011.11.042>.
50. J. Oh and G. TamizhMani, "Temperature testing and analysis of PV modules per UL 1703 and IEC 61730 standards," in *35th IEEE Photovoltaics Specialists Conf.*, pp. 000984–000988 (2010).
51. S. Bertho et al., "Improved thermal stability of bulk heterojunctions based on side-chain functionalized poly(3-alkylthiophene) copolymers and PCBM," *Sol. Energy Mater. Sol. Cells* **110**, 69–76 (2013), <http://dx.doi.org/10.1016/j.solmat.2012.12.007>.
52. S. Alem et al., "Effect of mixed solvents on PCDTBT: PC70BM based solar cells," *Org. Electron.* **12**(11), 1788–1793 (2011), <http://dx.doi.org/10.1016/j.orgel.2011.07.011>.
53. S. Cho et al., "A thermally stable semiconducting polymer," *Adv. Mater.* **22**(11), 1253–1257 (2010), <http://dx.doi.org/10.1002/adma.v22:11>.
54. B. Gholamkhass and P. Servati, "Solvent-vapor induced morphology reconstruction for efficient PCDTBT based polymer solar cells," *Org. Electron.* **14**(9), 2278–2283 (2013), <http://dx.doi.org/10.1016/j.orgel.2013.05.014>.
55. T. Wang, A. J. Pearson, and D. G. Lidzey, "Correlating molecular morphology with optoelectronic function in solar cells based on low band-gap copolymer: fullerene blends," *J. Mater. Chem. C* **1**(44), 7266–7293 (2013), <http://dx.doi.org/10.1039/c3tc31235f>.
56. W. R. Mateker et al., "Improving the long-term stability of PBDTTPD polymer solar cells through material purification aimed at removing organic impurities," *Energy Environ. Sci.* **6**(8), 2529–2537 (2013), <http://dx.doi.org/10.1039/c3ee41328d>.
57. K. Sivula et al., "Amphiphilic diblock copolymer compatibilizers and their effect on the morphology and performance of polythiophene: fullerene solar cells," *Adv. Mater.* **18**(2), 206–210 (2006), [http://dx.doi.org/10.1002/\(ISSN\)1521-4095](http://dx.doi.org/10.1002/(ISSN)1521-4095).
58. S. Ebadian et al., "Effects of annealing and degradation on regioregular polythiophene-based bulk heterojunction organic photovoltaic devices," *Sol. Energy Mater. Sol. Cells* **94**(12), 2258–2264 (2010), <http://dx.doi.org/10.1016/j.solmat.2010.07.021>.
59. E. Bundgaard et al., "Advanced functional polymers for increasing the stability of organic photovoltaics," *Macromol. Chem. Phys.* **214**(14), 1546–1558 (2013), <http://dx.doi.org/10.1002/macp.v214.14>.
60. J. Vandenbergh et al., "Thermal stability of poly[2-methoxy-5-(2'-phenylethoxy)-1,4-phenylenevinylene] (MPE-PPV): fullerene bulk heterojunction solar cells," *Macromolecules* **44**(21), 8470–8478 (2011), <http://dx.doi.org/10.1021/ma201911a>.
61. T. Lei, J.-Y. Wang, and J. Pei, "Roles of flexible chains in organic semiconducting materials," *Chem. Mater.* **26**(1), 594–603 (2014), <http://dx.doi.org/10.1021/cm4018776>.
62. B. J. Campo et al., "Ester-functionalized poly(3-alkylthiophene) copolymers: synthesis, physicochemical characterization and performance in bulk heterojunction organic solar cells," *Org. Electron.* **14**(2), 523–534 (2013), <http://dx.doi.org/10.1016/j.orgel.2012.11.021>.

63. D. M. Tanenbaum et al., “The ISOS-3 inter-laboratory collaboration focused on the stability of a variety of organic photovoltaic devices,” *RCS Adv.* **2**(3), 882–893 (2012), <http://dx.doi.org/10.1039/c1ra00686j>.
64. B. Andreasen et al., “TOF-SIMS investigation of degradation pathways occurring in a variety of organic photovoltaic devices—the ISOS-3 inter-laboratory collaboration,” *Phys. Chem. Chem. Phys.* **14**(33), 11780–11799 (2012), <http://dx.doi.org/10.1039/c2cp41787a>.
65. G. Teran-Escobar et al., “On the stability of a variety of organic photovoltaic devices by IPCE and in situ IPCE analyses—the ISOS-3 inter-laboratory collaboration,” *Phys. Chem. Chem. Phys.* **14**(33), 11824–11845 (2012), <http://dx.doi.org/10.1039/c2cp40821j>.
66. J. Kesters et al., “Enhanced intrinsic stability of the bulk heterojunction active layer blend of polymer solar cells by varying the polymer side chain pattern,” *Org. Electron.* **15**(2), 549–562 (2014), <http://dx.doi.org/10.1016/j.orgel.2013.12.006>.
67. P. R. T. Boudreault, A. Najari, and M. Leclerc, “Processable low-bandgap polymers for photovoltaic applications,” *Chem. Mater.* **23**(3), 456–469 (2011), <http://dx.doi.org/10.1021/cm1021855>.
68. J. E. Carlé et al., “Comparative studies of photochemical cross-linking methods for stabilizing,” *J. Mater. Chem.* **22**(46), 24417 (2012), <http://dx.doi.org/10.1039/c2jm34284g>.
69. C.-Y. Chang et al., “Enhanced performance and stability of a polymer solar cell by incorporation of vertically aligned, cross-linked fullerene nanorods,” *Angew. Chem.* **50**(40), 9386–9390 (2011), <http://dx.doi.org/10.1002/anie.v50.40>.
70. S.-O. Kim et al., “Thermally stable organic bulk heterojunction photovoltaic cells,” *Sol. Energy Mater. Sol. Cells* **95**(2), 432–439 (2011), <http://dx.doi.org/10.1016/j.solmat.2010.08.009>.
71. M.-H. Liao et al., “Morphological stabilization by supramolecular perfluorophenyl-C<sub>60</sub> interactions leading to efficient and thermally stable organic photovoltaics,” *Adv. Funct. Mater.* **24**(10), 1418–1429 (2013), <http://dx.doi.org/10.1002/adfm.201300437>.
72. Z. Li et al., “Performance enhancement of fullerene-based solar cells by light processing,” *Nat. Commun.* **4**, 2227 (2013), <http://dx.doi.org/10.1038/ncomms3227>.
73. A. Distler et al., “The effect of PCBM dimerization on the performance of bulk heterojunction solar cells,” *Adv. Energy Mater.* **4**(4), 1300693 (2014), <http://dx.doi.org/10.1002/aenm.201400171>.

Biographies of the authors are not available.